

Investigating the Effect of Bidispersity and Number of Particles on Stress

Michael E. Lasinski and Joseph F. Pekny
School of Chemical Engineering, Purdue University,
West Lafayette, IN 47907-1283, USA.
(lasinski, pekny)@ecn.purdue.edu

Jennifer S. Curtis
Chemical Engineering Department, University of Florida
Gainesville, FL 32611-6005, USA
jcurtis@che.ufl.edu

One limitation of Computational Fluid Dynamics based investigations of industrial scale particle flow phenomena is the inability to properly describe the effects of particle-particle interactions. Discrete element methods (DEM) present an opportunity to study such interactions. In flows with higher solids loadings these particle-particle interactions give rise to microstructure formation. Significant progress has been made in the investigation of the nature, size, and composition of the observed microstructure.¹ Recently DEM simulations have been used to investigate bidisperse systems with small numbers of particles.² In this work we simulate bidisperse systems containing much larger system sizes with a computationally efficient DEM simulation.

Specifically, we investigate the dependence of stress on the number of particles N with a bimodal distribution in a 3-D shear flow simulation. For the case of a coefficient of restitution of 0.6 and a solids volume fraction of 0.3, the ratio of the particle diameters, R , is varied from 1.0 to 3.0. As has been previously reported, there is an observed upward drift in stress with increasing numbers of particles when R equals 1.0. The upward drift occurs after the stresses appear to reach asymptotic behavior for small N . As R is increased, a similar upward drift in the stress is observed, however the effect is less pronounced because the overall magnitude of the stress decreases as R is increased. Previously reported clustering phenomena, observed in monodisperse systems, are also present in bidisperse systems. Also the effect of an increase in R on the initial onset of the increase in stress is investigated. Furthermore, the case of coefficient of restitution of 0.8 and solids volume fraction of 0.3 is studied in order to examine the effect of varying the coefficient of restitution. Finally, graphical visualizations of each simulation are used to illustrate the change in the system as N becomes large and to investigate number and size segregation effects as R increases.

¹ Lasinski, M. E., Pekny, J. F., Curtis, J. S., *Physics of Fluids*, **16** (2), 2004, 265-273

² Clelland, R., Hrenya, C. M., *Physical Review E*, **65**, 2002, 031301

I. Background

Processes containing both a solid particulate phase and a fluid phase are much more complicated than those only containing a fluid phase. Furthermore experiments are often difficult to implement due to the solid phase. As a result, computational fluid dynamics (CFD) models have been used to investigate industrial scale particle-phase phenomena in order to reduce the amount of required experimentation. Eulerian-Eulerian versions of these models require equations and hence closure relations for both the fluid phase and the solids phase. While the fluid phase relations are reasonably understood, the closure relations for the solids phase often yield models that do not accurately exhibit the particle-phase phenomena that has been observed experimentally. Furthermore, these models have difficulty predicting the particle-phase stress over a range of conditions.¹ Part of the problem is that the closure relations developed from previous approaches do not take into account individual particle-particle interactions.¹ Discrete Element Method (DEM) simulations represent a means to incorporate the effects of individual particle-particle interactions into CFD closure relations. As a first step, Liss and Glasser confirmed that the particle-phase stress does vary with system size.²

It remains to be determined how large of a system, in terms of number of particles, is required for this approach. If the system is too small, then it will not exhibit the particle-phase phenomena or microstructure formation that would occur in a large-scale process. There is ample evidence that in a simulation, there will be significant variation in the observed microstructure. For 2-D shear flow of 20,000 particles at a coefficient of 0.6, Tan and Goldhirsch observed no significant microstructure formation.⁵ Once they increased the system size to 200,000 particles, they observed clusters oriented at 45° .⁵ Furthermore, in low coefficient of restitution 3D shear flow simulations, Hopkins et al. observed alternating regions of low and high particle density.⁶ Lasinski et al. observed similar clustering phenomena in 3D simulations that were performed over a range of solids volume fractions and coefficient of restitutions.³ In addition, they identified that the clustering phenomena becomes more pronounced as the system size is increased and they conducted a preliminary investigation into the structure of the observed clusters. Furthermore they identified that the emergence of the clustering formation coincides with an additional increase in the particle-phase stress.³

Despite a continuing need to investigate monodisperse microstructure formation and particle-phase stress variation, there has recently been a trend towards studying bidisperse and continuous systems. There has already been a significant amount of bidisperse and continuous DEM simulation studies on systems with small numbers of particles. Clelland and Hrenya conducted 2D bidisperse shear flow simulations⁴ that showed relatively good agreement with the kinetic theory predictions of Willits and Arnarson at high values of the coefficient of restitution.⁷ Alam and Luding also performed 2D bidisperse shear flow simulations that showed good agreement with kinetic theory predictions.⁸ Both simulation studies suggested that the equipartition assumption begins to break down as e is decreased.⁸ Karion and Hunt carried out 2D bidisperse walled shear-flow simulations of systems with area fractions of 0.75.⁹ Dahl et al. have studied various continuous systems in both 2D and 3D.¹⁰⁻¹² Conway and Glasser examined the effect of polydispersity on the microstructure formation they observed in walled shear-flow simulations.¹³ In this paper, we continue the investigation into particle-phase stress increases and microstructure formation that was conducted for monodisperse systems by Lasinski et al.³ In addition we perform simulations at coefficients of restitution lower than those commonly used in previous bidisperse simulation studies.^{4, 8, 10-12}

II. Simulation and Conditions

In general, for all sets of conditions, a 3D cubic hard sphere DEM simulation is used. The shearing is maintained by Lees-Edwards boundary conditions with velocities of $+U$ and $-U$. As shown in Figure 1, the shearing is in the X-dimension, with the Lees-Edwards boundaries representing the upper and lower X-Z planes of the system. More details about the simulation method and the algorithmic modifications that allow for large numbers of particles are presented in Lasinski et al.³ However, that research only examined monodisperse systems. Therefore, there are some modifications to the simulation method and to the

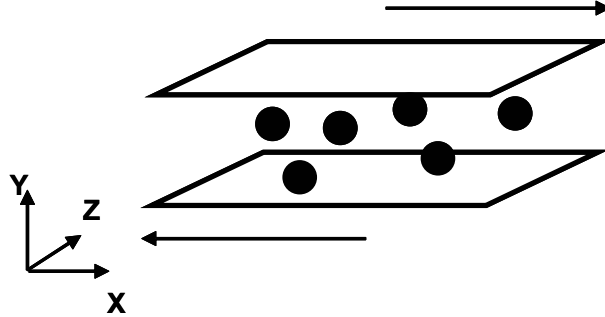


Figure 1: Simulation Axes

averaged calculations that are necessary in order to account for the bidispersity. The first is that the cell index method discussed in IIC of Lasinski et al.³ is modified so that the characteristic length of the cell is equal to the diameter of the larger particle (as opposed to that of the smaller particle). For large ratios of bidispersity, or R , the algorithmic benefits of the cell index method will clearly decrease. The second modification is in the calculation of the kinetic stress. In the monodisperse case the system is broken up into a number of averaging strips across the Y-dimension depending on system size. Averaged properties such as the kinetic stress are calculated locally in each strip. Then, if necessary, they are averaged across all of the strips. In the monodisperse case, the kinetic stress, τ_{strip}^k , is calculated using equation 1 where ρ_p is the particle density, ϕ is the solids volume fraction, and C is a particle's velocity deviation from the mean strip velocity.² In the bidisperse case, it is

$$\tau_{strip}^k = \rho_p \phi \langle CC \rangle \quad (1)$$

necessary to move the particle mass into the equation, similar to the method adopted by Dahl et al.¹⁰ In this case the kinetic stress is instead calculated using equation 2, where m_i is the mass of particle i , C_i is particle i 's velocity deviation from the average. L_j is the

$$\tau_{strip}^k = \frac{1}{L_X L_Y L_Z} \sum_{i=1}^{N_{strip}} m_i C_i C_i \quad (2)$$

j th directional length of a strip, N_{strip} is the number of particles in that strip. The stress is non-dimensionalized by dividing by $\rho_p d_L^2 \gamma^2$, where γ is the shear rate $2U/L$ and d_L is the diameter of the larger particle size in the simulation. The collisional stress is calculated using the same relation in Lasinski et al.³, except that d_p , the monodisperse particle diameter, is replaced by the average of the two particle diameters involved in the collision.

Simulations were performed for two sets of solids volume fractions, ϕ , and coefficients of restitution, e . Specifically they are (1) $e = 0.6$, $\phi = 0.3$ and (2) $e = 0.8$, $\phi = 0.3$. For each of the two sets of conditions, simulations were conducted for R , the ratio of particle diameters,

ranging from 1.25 to 3. N for each set of e , ϕ , and R , range from 250 to 40,000. Furthermore in all of the cases, there is an equal volume of large particle and small particles. Therefore there are significantly more smaller particles in each simulation.

III. Results and Discussion

For the first set of conditions, $e = 0.6$, $\phi = 0.3$, the stress appears to initially plateau at a specific value for small N simulations, as shown in Figure 2. As with the monodisperse case for $e = 0.6$, included from Lasinski et al.³, it is difficult to observe the first increase in stress up to the level of the initial plateau. It is only observable for $R = 2.0$. Furthermore, as R increases, up to 3.0, the particle-phase stress decreases for similar values of N .

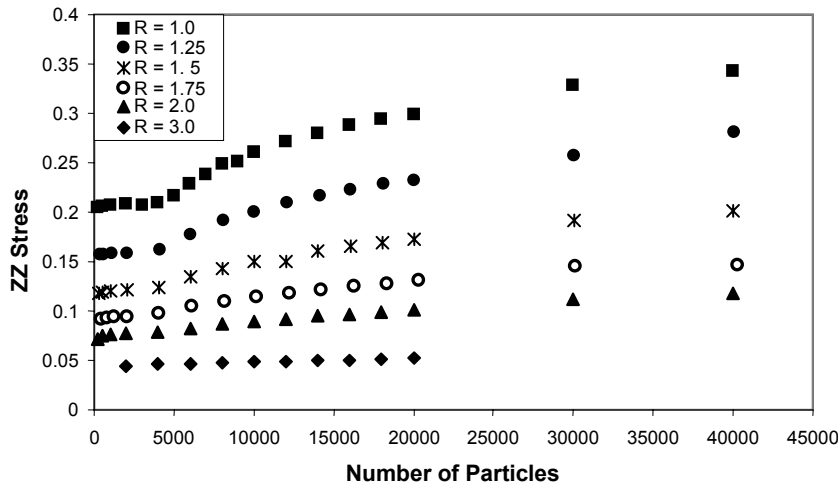


Figure 2: Dimensionless ZZ Normal Stress vs. Number of Particles ($e = 0.6$, $\phi = 0.3$)

As with the $R = 1$ (or monodisperse) case, after N is large enough, the particle-phase stress begins to increase to values significantly larger than the initial plateau values. It appears that the increase begins for all cases of R at roughly between 4000 and 6000 particles. However, that as R increases, there is less of a clear distinction between the first increase, the initial plateau, and the second increase. Furthermore as N increases up to 40,000, the particle-phase stress continues to increase.

For the case of $e = 0.8$, $\phi = 0.3$ similar trends, relative to the previous set of conditions are observed, as shown in Figure 3. As in the $e = 0.6$, $\phi = 0.3$ case, the particle-phase stress initially increases with N until it plateaus after only a small increase in N . In this case, the initial increase in stress is observable for $R = 2.0$. This suggests that as R increases, a larger simulation is required before the stress plateaus at the kinetic theory value. As before, the particle-phase stress then increases again once N has passed a certain threshold. In addition, as with the monodisperse case the second increase occurs at a larger system size for these conditions than it does for the $e = 0.6$, $\phi = 0.3$ case. Therefore variation of the coefficient of restitution has a similar affect for bidisperse systems as it does for monodisperse systems. However, increases in R , appear to decrease the threshold value of N for the second increase in stress. For the monodisperse case, the second increase in stress begins between $N = 18,000$ and $N = 20,000$. However, for $R = 1.25$, the increase in stress appears to begin at roughly $N = 16,000$ particles. For $R = 2.0$, the increase begins even earlier at $N = 12,000$. In

both cases, the particle-phase stress is still increasing after 40,000 particles. This would suggest, as in the monodisperse case, that larger systems are required before these results can be applied towards improving CFD models.

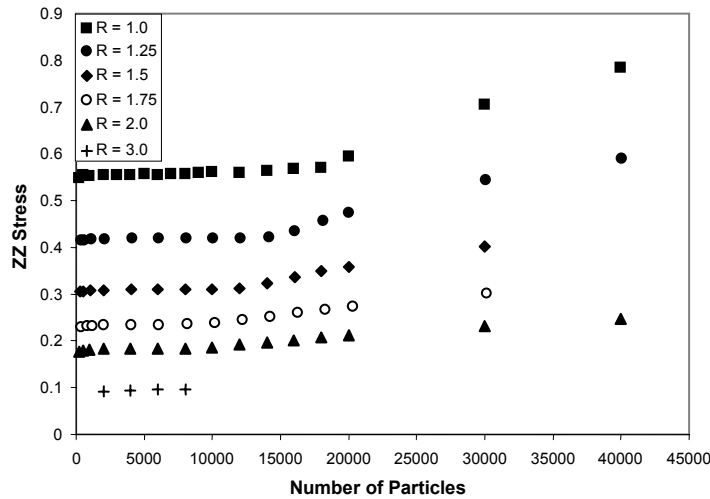


Figure 3: Dimensionless ZZ Normal Stress vs. Number of Particles ($\epsilon = 0.8, \phi = 0.3$)

As with the monodisperse results, there is again a change in the observable particle-phase phenomena once the stress starts to increase. However, the clustering, illustrated in the previous work, is shown using slices in the X-Y plane.³ In this work, the clustering is shown using pictures of the entire system, presented in the Y-Z plane, in order to illustrate the cluster structure. For example, for the conditions $\epsilon = 0.6, \phi = 0.3, R = 2.0$, Figures 4(a)-(c) show an evolution in the particle-phase phenomena, with system size, similar to that of the monodisperse case.³ In Figure 4(a), for $N = 4000$, the particles are evenly distributed about the system. Furthermore, the large and small particles are also evenly distributed about the system, with no sign of size segregation. In Figure 4(b), when $N = 6000$, there are both dense and dilute regions of particles. Despite the cluster formation, there is still no sign of size segregation. In Figure 4(c), when $N = 20,000$, the clustering is now more distinctly noticeable. A similar evolution in clustering phenomena is also observable for the conditions $\epsilon = 0.6, \phi = 0.3, R = 3.0$ as shown in Figure 5 (a)-(c). A similar emergence of a clustering phenomena also occurs for $\epsilon = 0.8, \phi = 0.3$. Furthermore, as in the monodisperse case the clusters do not persist across the width (or Z-dimension) of the system. As shown in Figure 4(b) and 4(c), there are clear changes in the clustering structure with variation in width. This is because the actual clusters stretch across the X-axis.

As shown in Figure 4, there is no clear evidence of segregation based on particle size. There is nothing akin to the segregation patterns observed in mixers.¹⁴ However there may be subtle segregation effects that are not observable. Furthermore this may also be because there are far less larger particles than smaller particles, so the segregation effects may not be as noticeable.

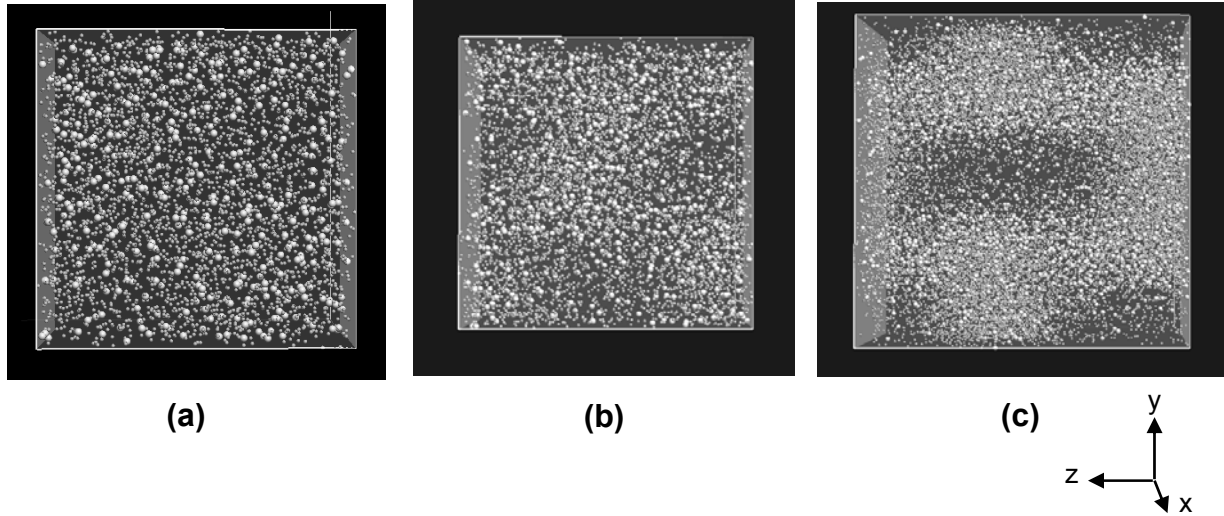


Figure 4: $e = 0.6$, $\phi = 0.3$, $R = 2.0$ (a) Slice of $N = 4000$, (b) $N = 10,000$, (c) $N = 20,000$

IV. Conclusions

In this paper, we have examined particle-phase stress variation with N for bidisperse systems. As with the monodisperse case, we have observed a similar increase in the particle-phase stress once a certain threshold number of particles has been reached. We have also observed that the degree of bidispersity also affects the transition between the initial increase in stress and the second increase in stress. In addition, we have observed similar cluster phenomena for bidisperse systems once N has reached a certain threshold depending on the conditions. As with the monodisperse results, further work is required to ascertain the particle-phase stress behavior for asymptotically large systems.

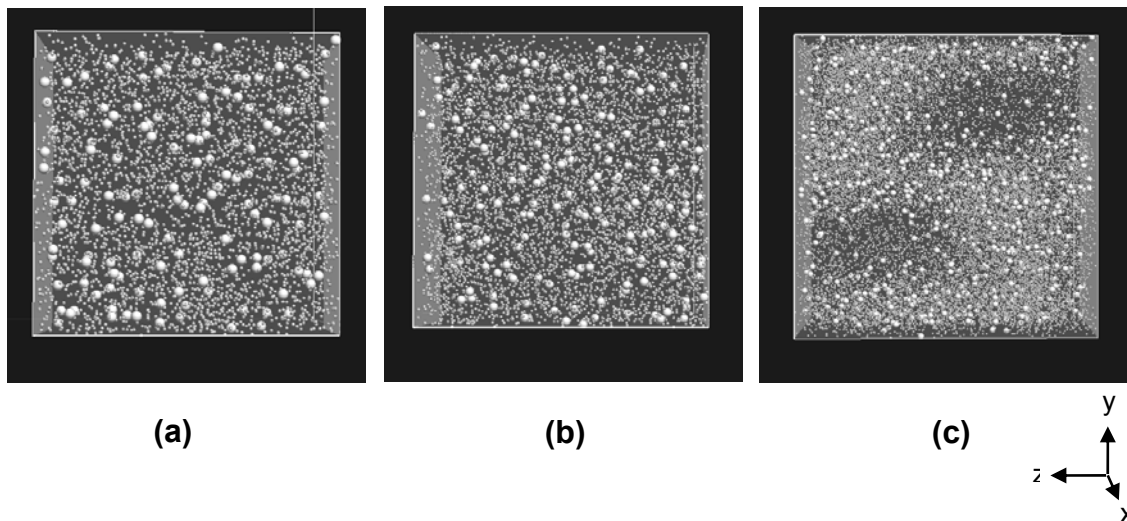


Figure 5: $e = 0.6$, $\phi = 0.3$, $R = 3.0$ (a) $N = 4000$, (b) $N = 10,000$, (c) $N = 20,000$

Acknowledgements

This work was supported in part by the Graduate Assistance in Areas of National Need Fellowship, by the NSF Industry/University Cooperative Center for Pharmaceutical Processing Research, and by Procter & Gamble. The images in Figures 4 and 5 were from the 3D real-time simulation software developed by Raj Arangarasan and Dat Nguyen at Purdue University's Envision Center for Data Perceptualization.

References

1. Hrenya, C. M., Sinclair, J. L., *Effects of Particle-Phase Turbulence in Gas-Solid Flows*, AIChE Journal, **43** (4), April 1997, 853-869
2. Liss, E. D., Glasser, B. J., *The Influence of Clusters on the Stress in a Sheared Granular Material*, Powder Technology, **116** (2), May 2001, 116-132
3. Lasinski, M. E., Pekny, J. F., Curtis, J. S., *Effect of System Size on Particle-Phase Stress*, Physics of Fluids, **16** (2), February 2004, 265-273
4. Clelland, R., Hrenya, C. M., *Simulations of a Binary-Sized Mixture of Inelastic Grains in Rapid Shear Flow*, Physical Review E, **65**, September 2002, 031301
5. Tan, M. L., Goldhirsch, I., *Intercluster Interactions in Rapid Granular Shear Flows*, Physics of Fluids, **9** (4), 856-869, 1997
6. Hopkins, M. A., Jenkins, J. T., Louge, M.Y., *On the Structure of Three-Dimensional Shear Flows*, Mechanics of Materials, **16**, 1993, 179-187
7. Willits, J. T., Arnarson, B. O., *Kinetic Theory of a Binary Mixture of Nearly Elastic Disks*, Physics of Fluids, **11** (10), October 1999, 3116-3122
8. Alam, M., Luding, S., *Rheology of Bidisperse Granular Mixtures via Event Driven Simulations*, J. Fluid. Mech., **476**, 2003, 69-103
9. Karion, A., Hunt, M., *Wall Stresses in Granular Couette Flows of Mono-Sized Particles and Binary Mixtures*, Powder Technology, **109** (1-3), April 2000, 145-163
10. Dahl, S. R., Clelland, R., Hrenya, C. M., *The Effects of Continuous Size Distributions on the Rapid Flow of Inelastic Particles*, Physics of Fluids, **14** (6), June 2002, 1972-1984
11. Dahl, S. R., Clelland, R., Hrenya, C. M., *Three-Dimensional, Rapid Shear Flow of Particles with Continuous Size Distributions*, Powder Technology, **138** (1), November 2003, 7-12
12. Dahl, S. R., Hrenya, C. M., *Size Segregation in rapid, granular flows with continuous size distributions*, Physics of Fluids, **16** (1), January 2004, 1-13
13. Conway, S., Glasser, B. J., *Density Waves and Coherent Structures in Granular Couette Flows*, Physics of Fluids, **16** (3), March 2004, 509-529
14. McCarthy, J. J., Ottino, J. M., *Particle Dynamics Simulation: A Hybrid Technique Applied to Granular Mixing*, Powder Technology, **97**, 1998, 91-99